PROCEEDINGS OF SCIENCE

Heavy flavor physics from lattice QCD

Takashi Kaneko[a,b,c,*]

[a] *Theory Center, Institute of Particle and Nuclear Studies, High Energy Accelerator Research Organization(KEK), Ibaraki 305-0801, Japan*

[b] *School of High Energy Accelerator Science, The Graduate University for Advanced Studies (SOKENDAI), Ibaraki 305-0801, Japan*

[c] *Kobayashi-Maskawa Institute for the Origin of Particles and the Universe, Nagoya University, Aichi 464-8602, Japan*

E-mail: takashi.kaneko@kek.jp

We review recent progress on heavy flavor physics from lattice QCD.

The 39th International Symposium on Lattice Field Theory (Lattice2022),
8-13 August, 2022
Bonn, Germany

[*] Speaker

PoS(LATTICE2022)238

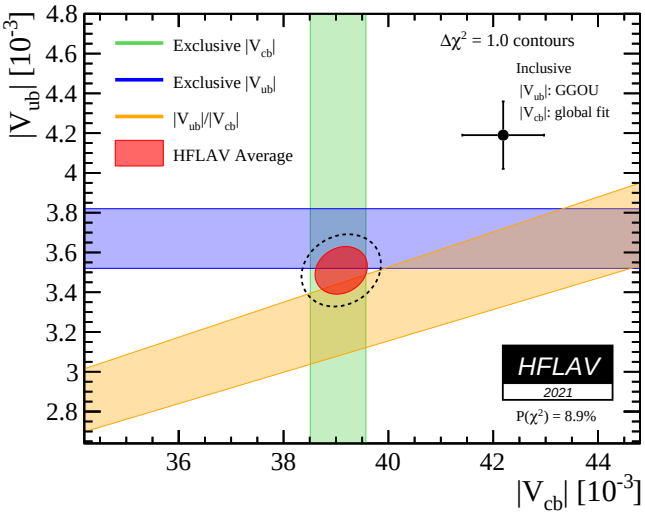

Figure 1: Recent estimate of CKM elements from exclusive (bands) and inclusive (black circle) (figure from Ref. [1]). The blue horizontal band shows $|V_{ub}|$ determined from $B \to \pi \ell \nu$, whereas the green vertical band is $|V_{cb}|$ determined from the $B \to D^{(*)} \ell \nu$ and $B_s \to D_s^{(*)} \ell \nu$ exclusive decays. The LHCb estimate of $|V_{ub}|/|V_{cb}|$ from $\Lambda_b \to p \mu \nu$ and $B_s \to K \mu \nu$ is also plotted by the slanted band. Their average (red region) is to be compared with the black circle from the inclusive decays.

1. Introduction

Heavy flavor physics provides an interesting testing ground of the Standard Model (SM) through various flavor changing processes of heavy hadrons. Indeed, theoretical and experimental investigations of B meson decays have reported intriguing tensions between the SM and experiments, so-called B anomalies, as hints of new physics beyond the SM. These includes tensions on the decay rate ratio $R(D^{(*)}) = \Gamma(B \to D^{(*)} \tau \nu)/\Gamma(B \to D^{(*)} \ell \nu)$ $(\ell = e, \mu)$ describing the lepton flavor universality violation (LFUV), the differential decay rate of the $B \to K \mu \mu$ decay and the angular distribution of the $B \to K^* \mu \mu$ decay.

These anomalies could be established as evidence of new physics together with on-going experiments, namely LHCb at CERN and SuperKEKB/Belle II at KEK. They play complementary roles in the search for new physics: LHCb accumulates large samples both for B and B_s mesons generated through high-energy proton collisions, whereas Belle II is an e^+e^- collider experiment of high efficiency and purity and, hence, advantageous in B decays to final states with neutrinos and/or multiple photons. Their physics run started in 2019 to accumulate fifty times more data than the previous KEKB/Belle experiment by the early 2030's. On the other hand, LHCb recently started Run 3, and a high luminosity upgrade (HL-LHC) is also planned.

However, there has been a long-standing problem in the determination of the Cabibbo-Kobayashi-Maskawa (CKM) matrix elements $|V_{ub}|$ and $|V_{cb}|$. As shown in Fig. 1, there is a tantalizing $\approx 3\,\sigma$ tension between analyses of the exclusive decays with the specified final state hadron(s) and the inclusive decays without such specification. While the tension can be explained by introducing a higher-dimensional tensor-type four fermion interaction beyond the SM, it largely distorts the $Z \to b\bar{b}$ decay rate, which has been precisely measured [2]. Therefore, it is likely that the tension is not due to new physics, but theoretical and/or experimental uncertainty has not been

fully understood. The largest theoretical uncertainty generally comes from relevant hadronic matrix elements.

Lattice QCD is a powerful framework to non-perturbatively calculate the hadronic matrix elements. There has been steady progress in the precise calculation of the so-called "gold-plated quantities", namely matrix elements for decays to the final state with at most one hadron stable in QCD. In addition, the past several years have witnessed challenges to the non-gold-plated processes especially for the inclusive decays relevant to the $|V_{ub}|$ and $|V_{cb}|$ tensions. In this article, we review such recent progress on the B and D meson decays. We refer the readers to Ref. [3] by Flavour Lattice Averaging Group (FLAG) for a comprehensive review and their world-average mainly on the gold-plated quantities. We also leave detailed discussions on the $B \to D^{(*)}\ell\nu$ decays to a dedicated review talk by Alejandro Vaquero at this conference [4].

2. Exclusive semileptonic decays

2.1 $B \to \pi\ell\nu$ decay

The $B \to \pi\ell\nu$ decay involving the light leptons $\ell = e, \mu$ provides the conventional determination of $|V_{ub}|$. As mentioned in the introduction, however, this shows $\gtrsim 2\ \sigma$ (12 %) tension with the inclusive analysis. This is a CKM suppressed process with the branching fraction of $\mathcal{B}(B \to \pi\ell\nu) \sim 1.5 \times 10^{-4}$ to be compared with $\mathcal{B}(B \to D^{(*)}\ell\nu)$ of several %. The accuracy of the previous Belle measurement is, therefore, limited by the statistics. It is expected to be largely improved by Belle II with the aimed integrated luminosity of $\int L \sim 50\, ab^{-1}$, which is fifty times larger than Belle. Actually, the "Belle II Physics Book" by Belle II-Theory Interface Platform (B2TiP) suggests that the accuracy of $|V_{ub}|$ would be limited by the uncertainty of lattice QCD at an early stage of Belle II around at $\int L \approx 10\, ab^{-1}$. In addition, $B \to \pi\tau\nu$ may provide a hint of new physics through the LFUV ratio $R(\pi) = \Gamma(B \to \pi\tau\nu)/\Gamma(B \to \pi\ell\nu)$ $(\ell = e, \mu)$, which is expected to be measured by Belle II with an accuracy of ≈ 14 %. It is, therefore, an urgent task to improve the lattice calculation of the $B \to \pi\ell\nu$ form factors. A target accuracy would be a few % or better in five years.

The recent status of the determination of $|V_{ub}|$ is summarized in the left panel of Fig. 2. Previous studies by the HPQCD [6], RBC/UKQCD [7] and Fermilab/MILC [8] Collaborations employed heavy quark actions based on effective field theories, such as the heavy quark effective theory (HQET) or non-relativistic QCD (NRQCD), to simulate around the physical bottom quark mass $m_{b,\mathrm{phys}}$. The best precision of ≈ 4 % has been achieved by Fermilab/MILC by simulating the lattice cutoffs $\lesssim 4.4$ GeV, pion masses down to $M_\pi \sim 165$ MeV and by using the so-called Fermilab approach, namely a HQET re-interpretation of the Wilson quark action [10]. Recently, the JLQCD Collaboration calculated the form factors through the relativistic approach using the Möbius domain-wall action [11] for all relevant quark flavors [9]. Their accuracy is typically 10 % at similar lattice cutoffs but with larger $M_\pi \gtrsim 230$ MeV. As seen in Fig. 2, therefore, the recent world averages of $|V_{ub}|$ have been dominated by the Fermilab/MILC study about seven years ago.

The uncertainty of the Fermilab/MILC, RBC/UKQCD and JLQCD calculations mainly comes from the statistics and continuum-chiral extrapolation. Controlling the chiral extrapolation is not easy for $B \to \pi\ell\nu$, because i) the chiral logarithm involves the $B^*B\pi$ coupling [12, 13], which can not be fixed from chiral symmetry, and ii), compared to $B \to D^{(*)}\ell\nu$, it is not suppressed by heavy

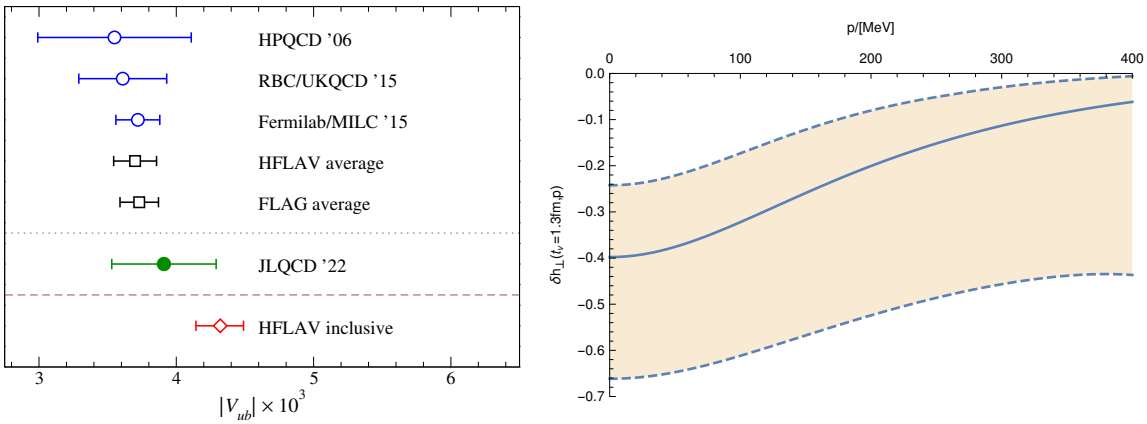

Figure 2: Left: comparison of recent estimate of $|V_{ub}|$ from $B \to \pi \ell \nu$. Blue open circles show previous estimates by the HPQCD [6], RBC/UKQCD [7] and Fermilab/MILC [8] Collaborations, whereas black open squares are obtained by HFLAV [1] and FLAG [3] using these lattice data. They are compared with recent JLQCD's estimate [9] (filled green circle), and $|V_{ub}|$ from the inclusive decay (red open diamond) [1]. Right: relative shift of $B \to \pi$ from factor $h_\perp$ as a function of pion momentum p (figure from Ref [21]). The time span of the intermediate $B^*\pi$ state is fixed to 1.3 fm.

quark symmetry [14, 15]. Therefore, we need a high statistics simulation close to the physical pion mass $M_{\pi,\text{phys}}$ to achieve the target accuracy comparable to the Belle II measurement. It is encouraging that Fermilab/MILC is pursuing a relativistic calculation using the highly improved staggered quark (HISQ) action on the MILC gauge ensembles covering the physical point $M_{\pi,\text{phys}}$ as well as the lattice cutoff $\lesssim 6.6$ GeV, where they may directly simulate the physical bottom mass $m_{b,\text{phys}}$ [16]. We also note that the RBC/UKQCD [17] and JLQCD studies are being updated.

However, there has been a concern about the (near-)physical point calculations of B meson observables: multi-particle states with additional pions give rise to non-negligible contamination as the pion mass decreases. Such excited state contamination to nucleon form factors has been carefully studied in Ref. [18], and similar contamination to B meson observables has been previously suggested by Shoji Hashimoto in his review at Lattice 2018 [19]. At this conference, Oliver Bär and Alexander Broll reported on the $B^*\pi$ state contamination to B meson observables within heavy meson chiral perturbation theory (ChPT) in the static limit [20, 21]. At the next-to-leading order (NLO), the relevant low energy constants (LECs) are those characterizing the B meson interpolating field and heavy-light vector current denoted by β_1 and β_2, respectively, as well as a linear combination of LECs in the NLO Lagrangian γ. Since these LECs are with the mass dimension -1 and not known, a conservative bound from a naive dimensional analysis is assumed as $-\Lambda_\chi^{-1} \le \beta_{1,2}, \gamma \le \Lambda_\chi^{-1}$, where $\Lambda_\chi \sim 1$ GeV is the cutoff scale of ChPT. The right panel of Fig. 2 shows the relative shift $\delta h_\perp$ to the form factor $h_\perp = \langle \pi(p)|V_k|B(0)\rangle/(2M_B p_k)$ in the HQET convention. They found volume-enhanced diagrams leading to a sizable contamination $\delta h_\perp$. Note that the differential decay rate for the light lepton channels $B \to \pi e \nu, \pi \mu \nu$ is described by the vector form factor f_+, a large fraction of which comes from $h_\perp$. Therefore, a more detailed investigation is necessary towards a precision determination of $|V_{ub}|$. To this end, the authors also proposed how to determine the NLO LECs from three- and two-point functions on the lattice.

The $B \to \rho \ell \nu$ decay is expected to provide an independent determination of $|V_{ub}|$ to resolve the tension with the inclusive decay. It also serves as new physics probe complementary to $B \to \pi \ell \nu$,

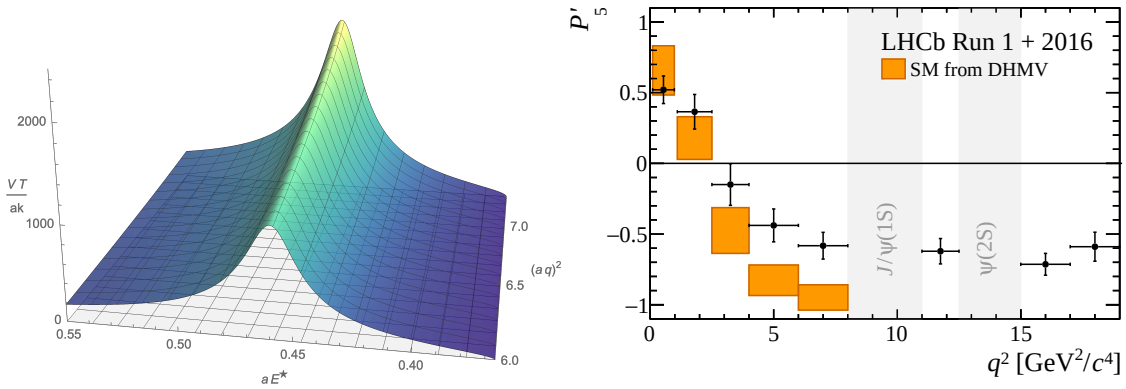

Figure 3: Left: $B \to \rho(\to \pi\pi)\ell\nu$ transition amplitude $\mathcal{A}$ through weak vector current (figure from Ref. [22]). The momentum transfer is denoted by q^2, and $E^\star$ represents the invariant mass of the $\pi\pi$ state.
Right: recent LHCb result for angular observable P_5' for $B \to K^*\ell\ell$ as a function of momentum transfer q^2 (figure from Ref. [26]). The black symbols show the LHCb result, which are compared with the orange band representing a SM prediction from Ref. [27]

since interactions with odd intrinsic parity can contribute. Luka Leskovec reported an interesting progress on this non-gold-plated mode [22]. They simulate $N_f = 2+1$ QCD with the clover light quarks and Fermilab b quarks on a $(3.6\,\mathrm{fm})^3$ box at $M_\pi \approx 320$ MeV, where ρ can decay into $\pi\pi$. In contrast to the previous quenched study [23], they calculate B meson three-point functions with sink operators of the single B state as well as $I=1$ $\pi\pi$ state to extract the ground-state contribution by generalized eigenvalue problem. Then, finite volume matrix elements of the weak vector and axial currents can be connected to the infinite volume transition amplitudes based on the formalism in Refs. [24, 25]. The left panel of Fig 3 shows their estimate of the $B \to \rho(\to \pi\pi)\ell\nu$ transition amplitude $\mathcal{A}$ through the weak vector current. While only the central value is available from the simulation at single combination of a and M_π, this is an encouraging progress towards an independent determination of $|V_{ub}|$ from $B \to \rho\ell\nu$. It is also interesting to extend this approach to the $B \to K^*\ell\ell$ decay, for which more than $3\,\sigma$ tension in its angular distribution has persisted for about ten years as shown in the right panel of Fig. 3.

2.2 B_s and B_c meson decays

The B_s and B_c meson semileptonic decays including $B_s \to D_s^{(*)}\ell\nu$, $B_c \to J/\Psi\ell\nu$ and $B_s \to K\ell\nu$, provide independent estimate of $|V_{ub}|$ and $|V_{cb}|$, as well as the LFUV ratios $R(X) = \Gamma(B_{s(c)} \to X\tau\nu)/\Gamma(B_{s(c)} \to X\{e,\mu\}\nu)$ as a probe of new physics. These modes have a few advantages on the lattice over the conventional $B \to \pi\ell\nu$ and $B \to D^{(*)}\ell\nu$ decays. First, they suffer from less statistical fluctuation. According to Lepage's analysis [28], the relative statistical error of the two-point function exponentially grows as the source-sink separation Δt increases

$$C_{\bar{Q}q} = \langle O_{\bar{Q}q}(\Delta t) O^\dagger_{\bar{Q}q}(0)\rangle, \qquad \frac{\delta C_{\bar{Q}q}}{C_{\bar{Q}q}} \propto e^{\alpha \Delta t}, \qquad \alpha = M_{\bar{Q}q} - \frac{M_{\bar{Q}Q} + M_{\bar{q}q}}{2}. \tag{1}$$

The exponent is significantly reduced by changing the spectator quark from u, d to s or c: for instance, $\alpha \simeq 0.60, 1.02, 0.24$ and 0.64 for the D, B, D_s and B_s, respectively. In addition, the chiral

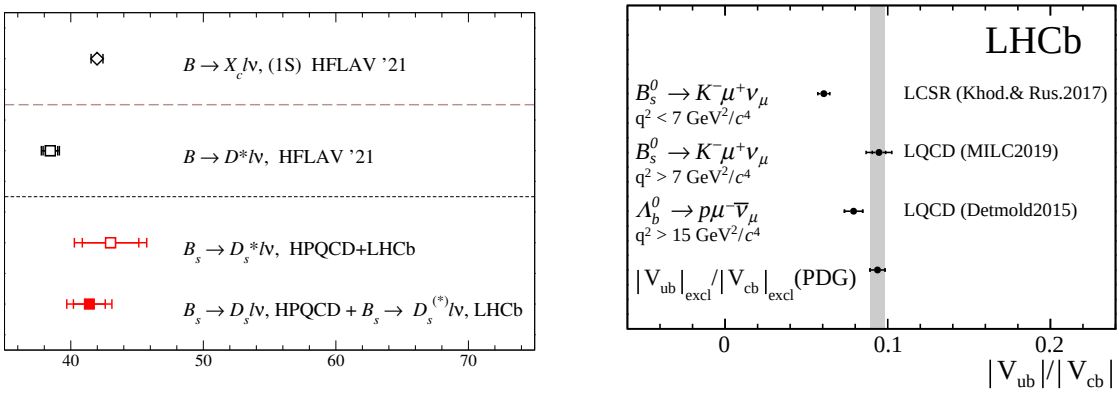

Figure 4: Left: comparison of $|V_{cb}|$ from semileptonic decays. The open red square is obtained by HPQCD's analysis of $B_s \to D_s^* \ell\nu$ [31], whereas the filled red square is from LHCb's analysis [32] of their data for $B_s \to D_s^{(*)} \ell\nu$ with theoretical input of HPQCD's $B_s \to D_s \ell\nu$ form factors [29]. These are compared with open black symbols obtained by the conventional exclusive ($B \to D^* \ell\nu$) and inclusive analyses[1].
Right: comparison of recent estimates of $|V_{ub}|/|V_{cb}|$ (figure from Ref. [40]). Two top symbols are from $B_s \to K\ell\nu$ and $B_s \to D_s \ell\nu$ using form factors from QCD light-cone sum rule [41] (top symbol) and from lattice QCD [39] (second top symbol). These are compared with estimates from $\Lambda_b \to p(\Lambda_c)\ell\nu$ [42] and conventional determination from $B \to \pi\ell\nu$ and $D^{(*)}\ell\nu$ [43].

extrapolation is expected to be better controlled with the reduced M_π dependence without valence pions. And, in some cases, the final state hadron with non-zero strangeness or charmness becomes stable under the strong interaction.

The HPQCD Collaboration has pursued the relativistic calculation of the $B_s \to D_s^{(*)} \ell\nu$ form factors with the HISQ heavy quarks [29–31]. As shown in Fig. 4, $B_s \to D_s^{(*)} \ell\nu$ currently allow us $\approx 5\,\%$ determination of $|V_{cb}|$, which is roughly three times worse than $B \to D^{(*)}\ell\nu$, and is consistent with both the conventional exclusive and inclusive analyses. We can, however, expect future improvement in both theory side (higher statistics on finer lattices) and experiment side (more data from LHCb Run-II and later). HPQCD also calculated the LFUV ratio for $B_c \to J/\Psi \ell\nu$ as $R(J/\Psi) = 0.258(4)$ [33]. This is consistent with the LHCb measurement $R(J/\Psi) = 0.71(25)$ [35]. The experimental uncertainty is expected to be largely reduced to $\delta R(J/\Psi) = 0.02$ by future "Upgrade II" of LHCb [36].

The $B_s \to K\ell\nu$ form factors have been calculated by HPQCD [37, 38], RBC/UKQCD [7] and Fermilab/MILC [39]. Recently, LHCb observed this CKM suppressed decay [40], and estimated $|V_{ub}|/|V_{cb}|$ from the ratio of the branching fractions $R_{\mathcal{B}} = \mathcal{B}(B_s \to K\ell\nu)/\mathcal{B}(B_s \to D_s\ell\nu)$. As shown in the right panel of Fig. 4, however, there is $\approx 4\,\sigma$ deviation between two estimates from different data sets: $R_{\mathcal{B}}$ at low $q^2 < 7$ GeV^2 with form factor input from QCD light-cone sum rule [41] and $R_{\mathcal{B}}$ at high $q^2 > 7$ GeV^2 with Fermilab/MILC's result for the form factors [39]. This may be attributed to the inconsistency among the form factor results shown in the left panel of Fig. 5. Independent realistic simulations are welcome to understand and resolve the discrepancy. Fermilab/MILC reported their on-going relativistic simulations with the HISQ heavy quarks at the lattice spacing down to 0.04 fm and the bottom quark mass $m_b \le 4m_c$ close to its physical value [16]. Preliminary result from their blinded analysis is shown in the same figure.

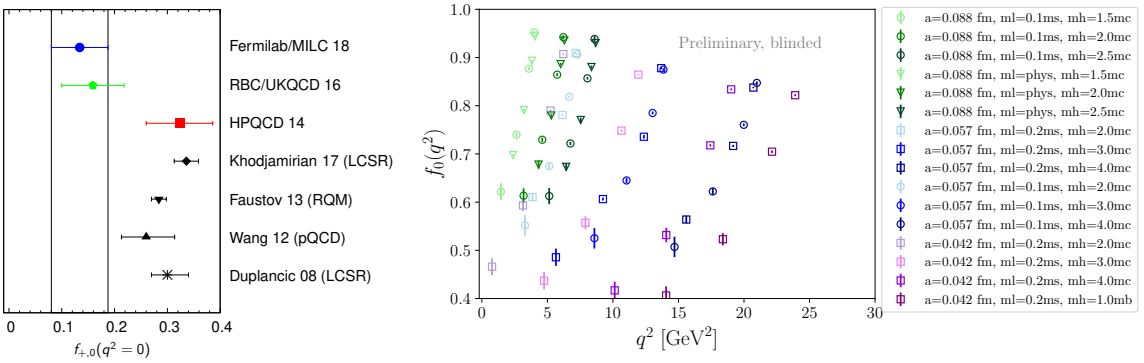

Figure 5:
Left: comparison of $B_s \to K$ vector and scalar form factor at zero momentum transfer $f_+(0) = f_0(0)$ at the time of 2019 (figure from Ref. [39]). The plot includes $f_+(0)$ from lattice QCD [7, 37, 39], QCD light-cone sum rule (LCSR) [41, 44] as well as those from relativistic quark model (RQM) [45] and NLO perturbative QCD [46].
Right: Fermilab/MILC's preliminary results for $B_s \to K$ scalar form factor $f_0(q^2)$ as a function of momentum transfer q^2 (figure from Ref. [16]). Different symbols show data at different lattice spacings, light quark masses and bottom quark masses. Note that these results are obtained from their blinded analysis.

3. Inclusive semileptonic decays

Let us consider the $B \to X_c \ell \nu$ inclusive decay where X_c collectively represents the hadron(s) with single charmness. The hadronic tensor $W_{\mu\nu}$ describes non-perturbative QCD effects to the differential decay rate

$$\frac{d\Gamma}{dq^2 dq^0 dE_\ell} = \frac{G_F^2}{8\pi^3}|V_{cb}|^2 L_{\mu\nu} W^{\mu\nu}, \tag{2}$$

where q^2 is the momentum transfer to the $\ell\nu$ pair, E_ℓ is the lepton energy in the B rest frame, and $L_{\mu\nu}$ is the leptonic tensor calculable perturbatively. Through the optical theorem and operator product expansion (OPE), $W_{\mu\nu}$ is expressed as the double expansion in the strong coupling α_s and inverse bottom quark mass m_b^{-1} with B meson matrix elements of local operators as non-perturbative input

$$\begin{aligned} W_{\mu\nu}(q) &= \sum_{X_c} (2\pi)^3 \delta^{(4)}(p-q-r) \frac{1}{2E_B} \left\langle B(p) \left| J_\mu^\dagger \right| X_c(r) \right\rangle \left\langle X_c(r) \left| J_\nu \right| B(p) \right\rangle \\ &\to \sum_i \frac{C(\alpha_s)}{m_b^{n_i}} \left\langle B \left| O_i \right| B \right\rangle, \end{aligned} \tag{3}$$

where J is the weak current, n_i is a positive integer depending on the operator O_i, and we suppress the argument p for $W_{\mu\nu}$ just for simplicity. Therefore, the analysis of the inclusive decay has very different systematics from that of the $B \to D^{(*)} \ell \nu$ exclusive decay. Hence comparison of the CKM elements between the exclusive and inclusive decays provides a rather non-trivial crosscheck, which we have not yet completed likely due to inadequate understanding of systematics.

Lattice QCD can provide the first-principles calculation of the non-perturbative inputs, such as $\mu_\pi^2(\mu) = (2M_B)^{-1}\langle B|\bar{b}D^2 b|B\rangle$ and $\mu_G^2(\mu) = (i/4M_B)\langle B|\bar{b}\sigma_{\mu\nu}G_{\mu\nu}b|B\rangle$ for $O(1/m_b^2)$ correc-

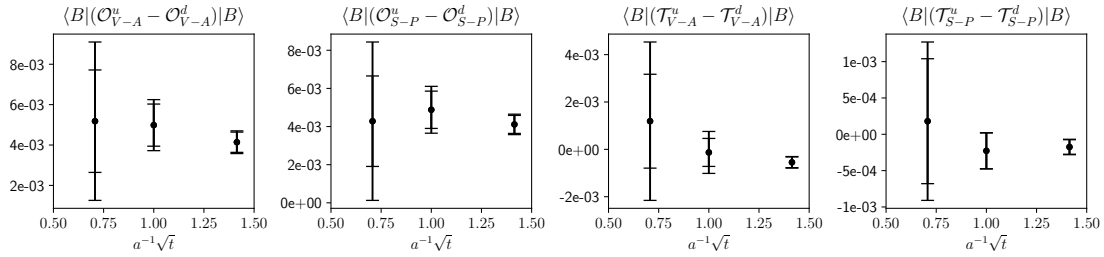

Figure 6:
Fit result for the bare matrix elements of dimension-6 operators as a function of Wilson flow time $\sqrt{t}$ (figure from Ref. [48]).

tions [47]. Joshua Lin reported their calculation of the matrix elements of the dimension-6 operators

$$\begin{aligned} O^q_{V-A} &= \left(\bar{b}\gamma_\mu P_L q\right)\left(\bar{q}\gamma^\mu P_L b\right), & O^q_{S-P} &= \left(\bar{b}P_L q\right)\left(\bar{q}P_R b\right), \\ T^q_{V-A} &= \left(\bar{b}\gamma_\mu P_L T^a q\right)\left(\bar{q}\gamma^\mu P_L T^a b\right), & T^q_{S-P} &= \left(\bar{b}P_L T^a q\right)\left(\bar{q}P_R T^a b\right) \end{aligned} \tag{4}$$

for $O(1/m_b^3)$ corrections to the heavy quark expansion [48]. Their matrix elements involving the light valence quark q describe the so-called spectator effects, which are responsible for the lifetime difference of beauty hadrons, such as $\tau(B^+)/\tau(B^0)$. They work in the static limit on RBC/UKQCD gauge ensembles at two lattice cutoffs $a^{-1} \simeq 1.8$ and 2.4 GeV and $M_\pi \gtrsim 300$ MeV. As shown in Fig. 6, they observe that both statistical and systematic errors of the fit to extract the matrix elements from relevant three- and two-point functions can be largely reduced by applying the Wilson flow [49] with the flow time $a^{-2}t = 0.5$, 1.0 and 2.0. Towards the application to the heavy quark expansion, the renormalization and continuum extrapolation are in progress.

In order to resolve the $|V_{cb}|$ and $|V_{ub}|$ tension, a direct lattice calculation of the inclusive decay rate is especially helpful, since it enables a detailed comparison between the inclusive and exclusive analyses in the same simulation. However, the B meson inclusive decay involves many non-gold-plated decay channels. The Lellouch-Lüscher formalism [50], which has been successfully applied to the $K \to \pi\pi$ decay [51], becomes increasingly intricate as the number of the relevant channels increases. At least currently, it is not straightforward to determine $W_{\mu\nu}(q)$ as a function of q.

Recent progress on the inclusive decay is based on an idea that it would be sufficient to evaluate an integral of $W_{\mu\nu}$ in order to estimate the relevant CKM element. Let us consider the spectral representation of the lattice four-point function

$$C_{\mu\nu}(t,\mathbf{q}) = \sum_{\mathbf{x}} \frac{e^{i\mathbf{q}\mathbf{x}}}{2M_B} \left\langle B(\mathbf{0}) \left| J^\dagger_\mu(\mathbf{x},t) J_\nu(\mathbf{0},0) \right| B(\mathbf{0}) \right\rangle = \int_0^\infty d\omega W_{\mu\nu}(\omega,\mathbf{q}) e^{-\omega t}, \tag{5}$$

where $\omega = q^0$. It is an ill-posed problem to determine $W_{\mu\nu}(\omega,\mathbf{q})$ from lattice data of $C_{\mu\nu}(t,\mathbf{q})$, because $W_{\mu\nu,L}$ at a finite lattice size L has a largely different functional form from $W_{\mu\nu}$ on the infinite volume : the multi-particle continuum part turns into a superposition of the δ function like singularities due to the discretized spectrum. Note also that, practically, a finite number of discrete data $C_{\mu\nu}$ are available with their statistical error. The basic idea of Ref. [52] is to determine a smeared spectral function

$$W_{\mu\nu,L,\sigma}(\omega') = \int_0^\infty d\omega \Delta_\sigma(\omega',\omega) W_{\mu\nu,L}(\omega), \tag{6}$$

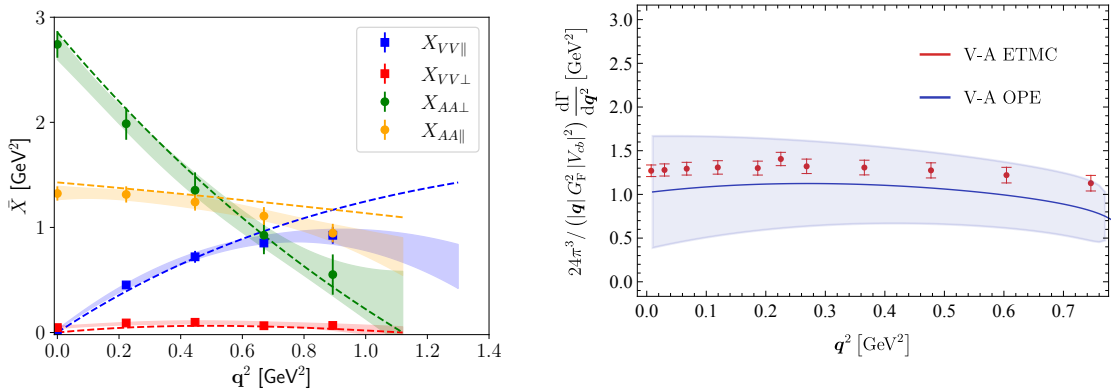

Figure 7: Left: comparison of $\bar{X}_{L,\sigma\to 0}(\mathbf{q}^2)$ with that from exclusive decay. Symbols and bands show $\bar{X}_{L,\sigma}(\mathbf{q}^2)$ in Eq. (7) for the $B_s \to X_{sc}\ell\nu$ inclusive decay in the $\sigma \to 0$ limit. Different symbols show data with different choices of the weak currents (vector or axial vector) and their polarization (perpendicular or not-perpendicular to $\mathbf{q}$) for $C_{\mu\nu}$. These are compared with the ground state contribution from the $B_s \to D_s^{(*)}\ell\nu$ exclusive decay (dased lines). All data are calculated on a JLQCD ensemble at $a^{-1} \approx 3.6$ GeV and $M_\pi \approx 300$ MeV [9].
Right: comparison of $\bar{X}_{L,\sigma\to 0}(\mathbf{q}^2)$ with conventional OPE calculation. The red circles are calculated on an ETM ensemble at $a^{-1} \approx 2.5$ GeV and $M_\pi \approx 400$ MeV [58]. The OPE prediction includes power corrections up to and including $O(1/m_b^{2,3})$ and $O(\alpha_s)$. (The left and right panels are taken from Ref. [56].)

where the smearing function $\Delta_\sigma(\omega', \omega)$ is a smooth approximation of the δ function: namely, $\lim_{\sigma\to 0}\Delta_\sigma(\omega', \omega) = \delta(\omega' - \omega)$. Estimating the smooth function $W_{\mu\nu,L,\sigma}(\omega')$ from $C_{\mu\nu}$ is a well-posed problem. The infinite volume spectral function is given by the double limit $W_{\mu\nu}(\omega) = \lim_{\sigma\to 0}\lim_{L\to\infty} W_{\mu\nu,L,\sigma}(\omega)$, where the order of the limits is not commutable. We refer the reader to the review talk by John Bulava for more details and interesting applications of this approach [53].

In Ref. [54], Paolo Gambino and Shoji Hashimoto proposed a method more directly applicable to the inclusive processes. Instead of the smearing function $\Delta_\sigma(\omega', \omega)$, the ω-integral kernel dictated by the kinematical factor and leptonic tensor in Eq. (2) is used to directly evaluate the inclusive rate

$$\Gamma = \frac{G_F^2}{24\pi^3}|V_{cb}|^2 \int_0^{\mathbf{q}^2_{\rm max}} d\mathbf{q}^2 \sqrt{\mathbf{q}^2}\bar{X}(\mathbf{q}^2), \quad \bar{X}_{L,\sigma}(\mathbf{q}^2) = \int_{\omega_{\rm min}}^{\omega_{\rm max}} d\omega K_{\mu\nu,\sigma}(\omega, \mathbf{q}^2) W_{\mu\nu,L}(\omega, \mathbf{q}^2), \quad (7)$$

where $w_{\rm min} = \sqrt{M_D^2 + \mathbf{q}^2}$ and $w_{\rm max} = M_B - \sqrt{\mathbf{q}^2}$. Note that $K_{\mu\nu}$ involves the Heaviside step function $\theta(\omega_{\rm max} - \omega)$ to realize the upper limit of the ω-integral. This is approximated by a smooth function, for instance a sigmoid function $\theta_\sigma(x) = 1/(1 + e^{-x/\sigma})$, in $K_{\mu\nu,\sigma}$. Therefore, the double limit $\bar{X}(\mathbf{q}^2) = \lim_{\sigma\to 0}\lim_{L\to\infty}\bar{X}_{L,\sigma}(\mathbf{q}^2)$ must be taken also in this method. We note that, as discussed in Ref.[55], this method can be applied to other inclusive processes, such as the charged current neutrino-nucleon scattering important for the neutrino experiments, by appropriately choosing the integral kernel.

At this conference, Antonio Smecca [57] reported on their feasibility study of the latter method [56]. They studied the computationally inexpensive $B_s \to X_{cs}\ell\nu$ inclusive decay, and made a detailed comparison among the conventional OPE calculation and lattice results obtained on ETM and JLQCD ensembles. The left panel of Fig. 7 compares the JLQCD data of

Table 1: Total width divided by $|V_{cb}|^2$ obtained from OPE and lattice calculations (results from Ref. [56]).

m_b/m_c	~ 2.4		~ 2.0	
	JLQCD	OPE	ETM	OPE
$\Gamma/\|V_{cb}\|^2 \times 10^{13}$ [GeV]	4.46(21)	5.7(9)	0.987(60)	1.20(46)

$\bar{X}_{L,\sigma}(\mathbf{q}^2) = (24\pi^3|\mathbf{q}|/G_F^2|V_{cb}|^2)(d\Gamma/d\mathbf{q}^2)$ appearing in Eq. (7) in the $\sigma \to 0$ limit. They observe good consistency between the full inclusive contribution of $B_s \to X_{cs}\ell\nu$ and its ground state contribution from the $B_s \to D_s^{(*)}\ell\nu$ exclusive decay. Note that these JLQCD data are obtained by using relativistic domain-wall bottom quarks with an unphysically small $m_b \simeq 2.44 m_c$ corresponding to $M_{B_s} \sim 3.5$ GeV. The authors discussed that the ground state saturation can be expected from the limited phase space as well as heavy quark symmetry due to the small m_b close to the charm mass m_c. The good consistency, therefore, demonstrates the validity of the inclusive analysis with very different systematics (for instance, the use of the $B_s \to B_s$ four-point function $C_{\mu\nu}$, and the approximated kernel $K_{\mu\nu,L,\sigma}$) from the exclusive analysis.

In the right panel of Fig. 7, on the other hand, the ETM data of $\bar{X}_{L,\sigma\to 0}(\mathbf{q})$ are compared with the conventional OPE calculation including $O(1/m_b^3)$ and $O(\alpha_s)$ corrections. The ETM data are also obtained at unphysically small $m_b \approx 2m_c$, but note that the comparison with the OPE can be made directly at the simulated m_b. They observe a reasonable consistency in $\bar{X}_{L,\sigma\to 0}(\mathbf{q}^2)$, which persists to the total rate $\Gamma/|V_{cb}|^2$ after integrating over $\mathbf{q}^2$ as shown in Table 1. However, they also observe tensions between lattice and OPE calculations through the decomposition into the vector and axial vector components as well as the perpendicular and longitudinal polarization components of $\bar{X}_{L,\sigma\to 0}(\mathbf{q}^2)$. This could be a manifestation of the violation of the quark-hadron duality, and hence deserves more detailed investigation in the future.

To that end, we need to more carefully study the systematics of this approach. As mentioned, the step function $\theta(x)$ in the ω-integration kernel $K_{\mu\nu}$ in Eq. (7) is approximated by a smooth function $\theta_\sigma(x)$, which goes to $\theta(x)$ in the $\sigma \to 0$ limit. In order to evaluate the ω-integral using lattice data $C_{\mu\nu}(t)$, we further approximate the smooth kernel $K_{\mu\nu,\sigma}$ with polynomials in $e^{-\omega}$ [54]. To this end, there have been two proposals. References [52, 60] proposed to use the so-called Backus-Gilbert method [61, 62]. It approximates $K_{\mu\nu,\sigma}$ with the basis functions $b_t(\omega) = e^{-\omega t}$ as

$$K_{\mu\nu,\sigma} \simeq \sum_t^N g_t b_t(\omega), \tag{8}$$

where the coefficients $\{g_t\}$ are determined by minimizing the norm

$$\int_{\omega_0}^{\infty} d\omega |K_{\mu\nu,\sigma} - \sum_t^N g_t b_t(\omega)|^2, \tag{9}$$

as long as the polynomial approximation is concerned. Another proposal [54] employs the (shifted) Chebyshev polynomial $T_j^*(e^{-\omega t})$ as

$$K_{\mu\nu,\sigma} \simeq \frac{c_0^*}{2} + \sum_k^N c_k^* T_k^*(e^{-\omega t}), \tag{10}$$

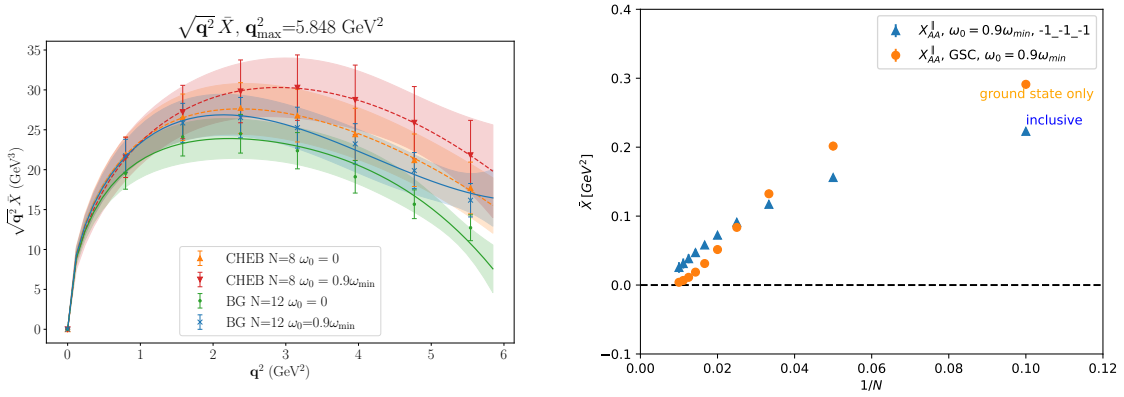

Figure 8: Left: comparison of $\sqrt{\mathbf{q}^2}\bar{X}_{L,\sigma}(\mathbf{q}^2)$ between Backus-Gilbert method and Chebyshev approximation as well as different values of ω_0 (figure from Ref. [59]). All data are calculated on a RBC/UKQCD ensemble at $a^{-1} \approx 1.8$ GeV and $M_\pi \approx 330$ MeV.
Right: axial vector component $X^{\parallel}_{AA,L,\sigma}(\mathbf{q}^2)$ of $\bar{X}_{L,\sigma}(\mathbf{q}^2)$ as a function of $1/N = \sigma$ (figure from Ref. [64]). The blue triangles show the full inclusive result, whereas the orange circles are its ground state contribution.

where the maximum deviation is minimized (the min-max approximation). We note that t in these approximations is identified with the argument of $C_{\mu\nu}(t)$ to evaluate the ω-integral.

Alessandro Barone *et al.* carried out a systematic study on this approximation step. The ω integral $\sqrt{\mathbf{q}^2}\bar{X}_{L,\sigma}(\mathbf{q}^2)$ is evaluated by using the Backus-Gilbert and Chebyshev approaches as well as by varying ω_0, which is the lower cut of the ω-region to approximate $K_{\mu\nu,\sigma}$. They employ the relativistic heavy quark (RHQ) action [63] based on HQET to simulate the physical mass $m_{b,\text{phys}}$ on a RBC/UKQCD ensemble at $a^{-1} \simeq 1.8$ GeV. The reasonable consistency shown in the left panel of Fig. 8 demonstrates the stability of the inclusive analysis against the choice of the approximation method and ω-region thereof. We also note that their simulation at $m_{b,\text{phys}}$ may observe significant contribution of the excited states to the inclusive rate.

The same authors also studied another important systematics: namely, the extrapolation to the $\sigma \to 0$ limit and the associated uncertainty. As reported by Ryan Kellermann [64], on the JLQCD ensemble mentioned above, they focus on the $D_s \to X_{ss}\ell\nu$ inclusive decay, which can be precisely studied even through the relativistic approach, because all relevant valence quark masses can be set to their physical value with discretization effects under control. They observe that the σ extrapolation is essential to quantitatively estimate the differential decay rate. The right panel of Fig. 8 shows the axial current component $X^{\parallel}_{AA,L,\sigma}$ with their polarization non-perpendicular to $\mathbf{q}$. This receives the leading contribution from the $s\bar{s}$-vector state φ, since $\langle\eta_s|A_\mu|B\rangle$ vanishes due to parity symmetry. However, this also vanishes with the chosen momentum $\mathbf{q} = (1,1,1)$ (in units of $2\pi/L$), because $E_\varphi > M_{D_s}$. The figure shows that $X^{\parallel}_{AA}$ is not zero at large values of $\sigma = 1/N$ possibly due to the error of the kernel approximation, and it approaches to zero at $\sigma \lesssim 0.01$ suggesting the importance of the σ extrapolation.

They also provided an error estimate based on a mathematical property of the Chebyshev polynomial $|T^*_k(e^{-\omega t})| \le 1$, namely by assuming the mathematical upper and lower limits of T^*_k. This covering the ground state contribution could be too conservative, and further study for more realistic error estimate is needed. Another importance issue is approaching the infinite volume limit $L \to \infty$, which has not been studied for the application to heavy meson inclusive decays.

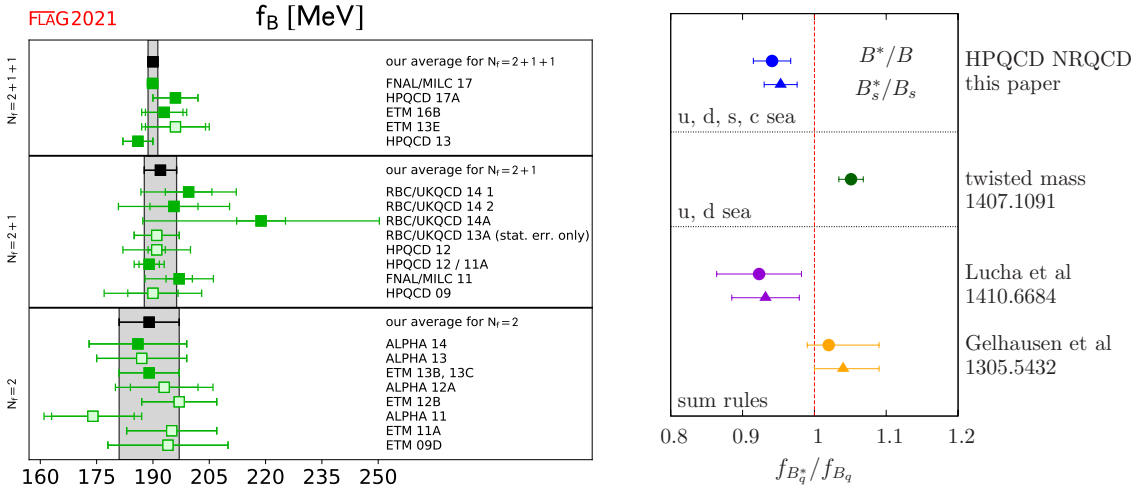

Figure 9: Left: comparison of realistic calculations of f_B (figure from the latest FLAG review [3]). The green squares are individual studies, whereas the black squares and bands represent their average for $N_f = 2+1+1$ 2+1 and 2.
Right: previous estimates of f_{B^*}/f_B (figure from Ref. [67]). The blue [67] and black [68] symbols show results from lattice QCD, whereas the purple [69] and orange [70] symbols are from QCD sum rules.

4. Leptonic decays

The $B \to \ell\nu$ leptonic decay provides an alternative determination of $|V_{ub}|$ as well as interesting probe of new physics sensitive only to odd parity interactions. Through many independent calculations shown in the left panel of Fig. 9, the relevant hadronic input, namely the decay constant f_B, is determined with the ≈ 0.7 % accuracy, at which the electromagnetic (EM) corrections would be no longer negligible. The accuracy of $|V_{ub}| = 4.05(3)_{\rm th}(65)_{\rm exp}$ [3] is, however, largely limited by the statistics of experimental data due to the helicity suppression. B2TiP suggests that the experimental uncertainty will be largely reduced to a few % at the target luminosity of Belle II, and $B \to \ell\nu$ will determine $|V_{ub}|$ with an accuracy competitive to $B \to \pi\ell\nu$.

The decay constant f_{B_s} of the neutral B_s meson describes the $B_s \to \mu\mu$ decay, which is mediated by the flavor changing neutral current (FCNC), and hence is expected to be sensitive to new physics. Previously, a combined analysis of the branching fraction $\mathcal{B}(B_s \to \mu\mu)$ by the ATLAS, CMS and LHCb experiments reported $\sim 2.1\,\sigma$ tension with the SM prediction [65], which, however, became insignificant in the latest CMS result [66]. Similar to f_B, many independent lattice calculations leads to the FLAG average with the 0.6 % accuracy leading to the theoretical precision of $\Delta\mathcal{B}(B_s \to \mu\mu) \sim 4$ %. This is better than the current experimental accuracy of $\sim$ 10 %, which is expected to become competitive to the SM precision by HL-LHC.

Having achieved the good precision for $f_{B_{(s)}}$, it is interesting to explore different observables. One direction is to extend to other mesons, such as B^* and B_c. In contrast to $f_{B_{(s)}}$, however, there have been much less studies of the vector meson decay constant f_{B^*} as shown in the right panel of Fig. 9. Due to the tension between the lattice studies, more independent studies are highly welcome. At this conference, RBC/UKQCD reported on their on-going study of f_{B^*} as well as f_{B_c} [71]. They simulate four lattice cutoffs up to $a^{-1} \sim 3.2$ GeV and pion masses down to $M_\pi \sim 270$ MeV with the RHQ action for bottom quarks. While the continuum extrapolation has

to be done, they observe reasonable signal and ground-state saturation for both the B^* mass and dimensionless decay amplitude $\Psi_{B^*}/M_{B_s}^{3/2} = f_{B^*}\sqrt{M_{B^*}}/M_{B_s}^{3/2}$ as shown in the left panel of Fig. 10.

Another interesting direction is to study the radiative leptonic decay $B \to \ell\nu\gamma$. This mode potentially provides an alternative determination of $|V_{ub}|$, since the helicity suppression is lifted with a photon in the final state, and Belle II is expected to measure the branching fraction $\mathcal{B}(B \to \ell\nu\gamma)$ with 4 % accuracy [5]. For large photon energy E_γ, this would be an clean probe of the internal structure of the B meson, for example the first inverse moment $1/\lambda_B$ of the light-cone distribution amplitude. The RM123+SOTON collaboration has studied the radiative decays $P \to \ell\nu\gamma$ of light mesons ($P = \pi$ and K) in the full region of the photon energy, and $D_{(s)} \to \ell\nu\gamma$ for soft photons ($E_\gamma \leq 400$ MeV). They employ the twisted mass discretization and simulate four lattice cutoffs up to $a^{-1} \leq 3.2$ GeV and pion masses down to $M_\pi = 220$ MeV.

At this conference, Davide Giusti reported their study of the K and $D_{(s)}$ radiative decays in full photon energy region aiming at an extension to $B \to \ell\nu\gamma$ [73]. The relevant correlators are calculated on a RBC/UKQCD ensemble at $a^{-1} \sim 1,8$ GeV and $M_\pi \simeq 340$ MeV. The matrix element is decomposed as

$$\begin{aligned} & -i \int d^4x e^{ip_\gamma x} \left\langle 0 \left| T\left[J_\mu^{(\mathrm{EM})}(x) J_\nu^{(\mathrm{weak})}(0) \right] \right| P(p_P) \right\rangle \\ = \; & \varepsilon_{\mu\nu\rho\sigma} p_\gamma^\rho \nu^\sigma F_V + i\left[-g_{\mu\nu} + \nu_\mu (p_\gamma)_\nu \right] F_A - i \frac{\nu_\mu \nu_\nu}{\nu p_\gamma} M_P f_P + (p_\gamma)_\mu\text{-terms}, \end{aligned} \tag{11}$$

where F_V, F_A and F_P represent the vector, axial vector and pseudo-scalar form factors, respectively. The last term represents the contributions proportional to $(p_\gamma)_\mu$, which vanishes when contracted with p_γ. For large photon energy, the decay amplitude is described by F_V and the structure dependent part of the axial vector form factor $F_{A,\mathrm{SD}} = F_A + Q_\ell F_P / E_\gamma$, where Q_ℓ is the lepton charge. Improved simulation techniques, such as the all mode averaging [74] and Z_2 noise wall-source, enable them to calculate both F_V and $F_{A,\mathrm{SD}}$ in the full kinematical region as shown in the right panel of Fig. 10. After their continuum and chiral extrapolation are completed, it would be interesting to make a detailed comparison with experiments.

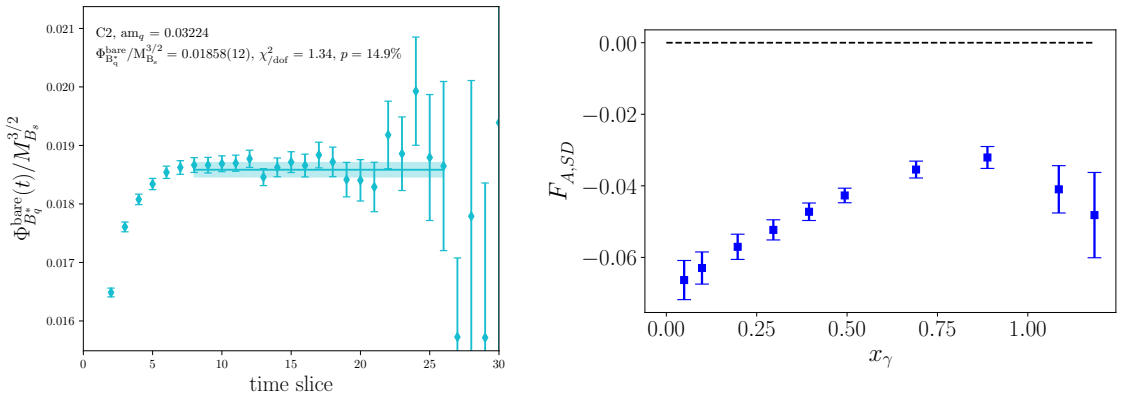

Figure 10: Left: effective plot of dimensionless decay amplitude $\Psi_{B^*}/M_{B_s}^{3/2} = f_{B^*}\sqrt{M_{B^*}}/M_{B_s}^{3/2}$ (figure from Ref. [71].)
Right: structure dependent part of axial vector form factor $F_{A,\mathrm{SD}}$ as a function of $x_\gamma = 2\nu p_\gamma / M_P$ (figure from authors of Ref. [73]).

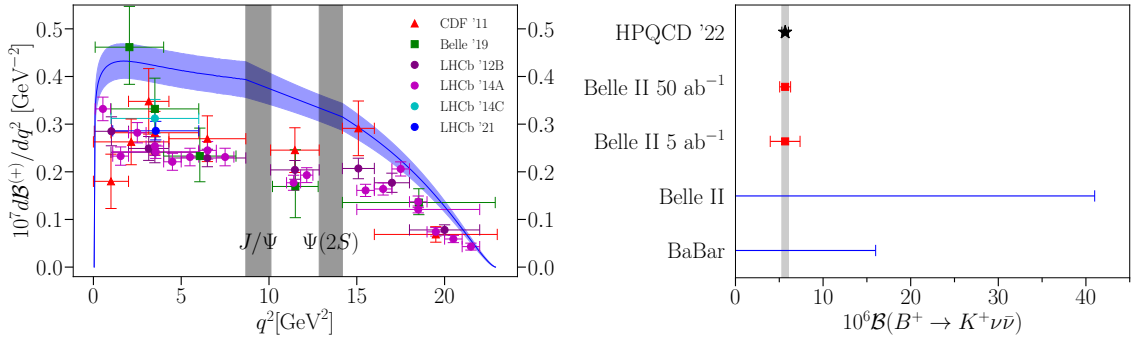

Figure 11: Left: differential branching fraction $d\mathcal{B}/dq^2$ for $B \to K\ell\ell$. HPQCD estimate (blue band) is compared with experimental data shown by symbols.
Right: branching fraction of $B \to K\nu\nu$. HPQCD estimate is compared with the recent Belle and Belle II measurements as well as the expected accuracy for Belle II. (Both panels are from Ref. [77].)

5. FCNC processes

The B meson processes mediated by the FCNC, such as the neutral $B_{(s)}$ meson mixing and $B_s \to \mu\mu$, occur only beyond the tree-level in the SM, and hence are sensitive to new physics. The long-standing tension in the angular distribution of $B \to K^*\ell\ell$ shown in the right panel of Fig. 3 is a famous example of the B anomalies. While it is not straightforward to simulate this non-gold-plated decay on the lattice, it would be interesting to extend the study of $B \to \rho(\to\pi\pi)\ell\nu$ discussed above. There has been a concern that the tension is due to the insufficient understanding of the non-perturbative effects from the nearby charmonium resonances J/Ψ and $\Psi(2S)$, namely $B \to J/\Psi(\to\ell\ell)K$. We note that Ref. [75] reported a lattice study of the factorization approximation used to study the long-distance charmonium effects.

On the other hand, it is straightforward to calculate the form factors for the gold-plated $B \to K\ell\ell$ decay. Recently, HPQCD performed a relativistic calculation of the vector, scalar and tensor form factors [76–78]

$$\langle K(p')|V_\mu|B(p)\rangle = \left\{P - \frac{\Delta M^2}{q^2}q\right\}_\mu f_+(q^2) + \frac{\Delta M^2}{q^2}q_\mu f_0(q^2), \tag{12}$$

$$\langle K(p')|T_{k0}|B(p)\rangle = \frac{2ip_0p'_k}{M_B + M_K} f_T(q^2), \tag{13}$$

where $P = p + p'$, $q = p - p'$ and $\Delta M^2 = M_B^2 - M_K^2$. With realistic parameters such as five lattice cutoffs up to $a^{-1} \sim 4.5$ GeV, pion masses down to the physical point $M_{\pi,\text{phys}}$, and m_b close to its physical value $m_{b,\text{phys}}$ ($m_b/m_{b,\text{phys}} \approx 0.8$), they calculate the form factors in the full kinematical range of q^2 with the typical accuracy of 4-7 % dominated by statistical error. As previously reported by Fermilab/MILC[79], theoretical estimate of the differential branching fraction $d\mathcal{B}(B \to K\ell\ell)/dq^2$ is systematically smaller than experiment as shown in Fig. 11. The previous $2\,\sigma$ tension is enhanced to $4.7\,\sigma$ with the precise HPQCD results. This favors a significant shift of the Wilson coefficients for the effective Hamiltonian operators $Q_9 = (e^2/16\pi^2)(\bar{q}_L\gamma b_L)(\bar{\ell}\gamma^\mu\ell)$ and $Q_{10} = (e^2/16\pi^2)(\bar{q}_L\gamma b_L)(\bar{\ell}\gamma^\mu\gamma_5\ell)$ from the SM.

The vector form factor describes the short distance contribution to the $B \to K\nu\nu$ decay as $d\mathcal{B}(B \to K\nu\nu)/dq^2|_{\text{SD}} \propto |V_{tb}V_{ts}^*|^2|\mathbf{p}'|^3 f_+(q^2)^2$. This decay can be used for the dark sector search,

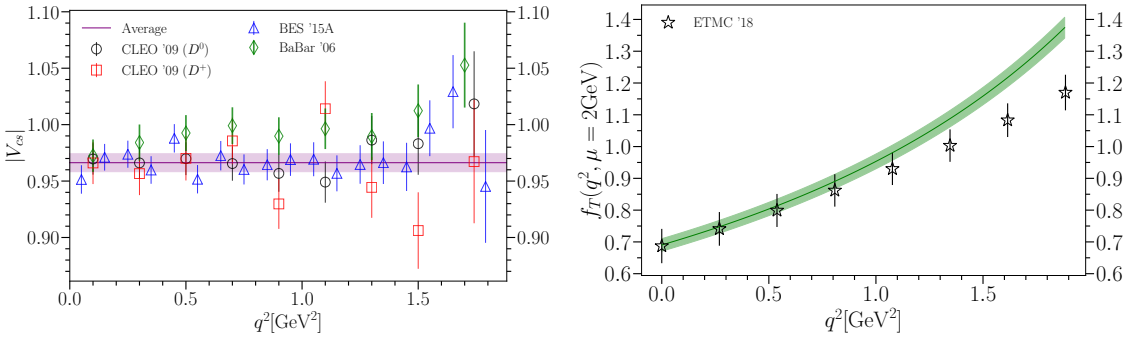

Figure 12: Left: $|V_{cs}|$ from comparison of differential decay rate between theory and experiment (figure from Ref. [83]).
Right: tensor form factor f_T as a function of q^2 (figure from Ref. [76]).

since it shares missing energy signature with $B \to K X_{\text{dark}}$ with invisible particle(s) X_{dark}. It is indeed suggested that Belle II is sensitive to dark scalar particles in the GeV range [80]. The right panel of Fig. 11 shows that i) recent Belle and Belle II measurements of the branching fraction is consistent with zero, ii) but it will be largely improved by Belle II, iii) and the theoretical prediction with the HPQCD's estimate of f_+ is already as accurate as the Belle II target accuracy.

6. $D_{(s)}$ meson decays

Recent precision lattice calculations of the $K \to \pi \ell \nu$ from factors and decay constant ratio f_K/f_π as well as better understanding of the radiative corrections to the superallowed nuclear β decays enable a precision test of CKM unitarity in the first row, which suggests $\gtrsim 3\,\sigma$ tension called the "Cabibbo angle anomaly" [3, 81]. It is natural to extend the precision test to the second row. Previously, the accuracy of $|V_{cs(d)}|$ from the $D \to K(\pi)\ell\nu$ semileptonic decay is limited by lattice calculation of the relevant form factors. On the other hand, experimental uncertainty dominates the error of $|V_{cs(d)}|$ from the leptonic decays due the helicity suppression [82].

Recently, HPQCD carried out a precision calculation of the $D \to K \ell \nu$ form factors by a fully realistic simulation: namely at five lattice cutoffs up to $\lesssim 4.5$ GeV and at physical light, strange and charm quark masses. As shown in the left panel of Fig. 12, the form factor shape is consistent with experimental data, and $|V_{cs}|$ is determined with the accuracy 1 %, where the theoretical and experimental uncertainties are comparable to each other. As a result, CKM unitarity is confirmed with a few % accuracy as $|V_{cd}|^2 + |V_{cs}|^2 + |V_{cb}| = 0.993(25)_{cd}(13)_{cs}$, where $|V_{cb}|$ is too small to significantly contribute to this test.

A more precise determination of $|V_{cd}|$ is the next target to improve this unitarity test. To this end, it is encouraging that RBC/UKQCD [84], ALPHA/CLS[85] and Fermilab/MILC[86] collaborations reported their preliminary and/or blinded analyses of $D \to \pi \ell \nu$. We note that Refs. [84, 86] also discuss an alternative determination of $|V_{cd}|$ through $D_s \to K \ell \nu$, which is expected to be advantageous on the lattice as discussed above.

There is, however, a concern about the $D \to K$ tensor form factor. As shown in the right panel of Fig. 12, there is about $3\,\sigma$ disagreement between recent determinations by HPQCD [76] and

ETM [87] around $q^2_{\rm max}$, where the lattice calculations are expected to be reliable. At this moment, this disagreement is difficult to understand, and more independent studies are necessary.

7. Summary

In this article, we reviewed recent progress on heavy flavor physics from lattice QCD. There has been steady progress in precisely calculating the gold-plated quantities by realistic simulations. A good accuracy has been already achieved for some of the experimentally challenging processes, for instance, helicity-suppressed leptonic decays (decay constants) and loop-suppressed FCNC decays ($B \to K\ell\ell, K\nu\nu$ form factors). For the exclusive semileptonic decays, on the other hand, more realistic simulations at physical quark masses and at large recoils as well as careful investigation of systematics, such as the ground state saturation, are needed to resolve the $|V_{ub}|$ and $|V_{cb}|$ tensions and to search for new physics. These are also helpful in resolving the existing tensions among lattice studies about f_{B^*}, $B_s \to K$ form factors at low q^2 and $D \to K$ tensor form factor at large q^2 likely due to inadequate understanding of systematics.

We stress that there has been remarkable progress in developing new applications to non-gold-plated processes. In particular, the inclusive decays attract much attention and the feasibility and systematics are being actively studied. Note also that the currently developed methods have wide applications beyond B physics, for instance, to the inclusive τ decay and ℓN scattering. However, taking the infinite volume limit has not been tested well, and is important future subject towards realistic simulation of the inclusive B decays. There has been good progress also in the study on $B \to \ell\nu\gamma$, $B \to \rho(\to \pi\pi)\ell\nu$ and life time difference. The remaining challenging subjects include an extension to long distance contributions to $B \to K^*\ell\ell$, D mixing and QCD based study of the factorization.

I thank O. Bär. A. Barone, A. Broll, M. Black, C.T.H. Davies, J. Frison, D. Giusti, S. Hashimoto, W. Jay, A. Jüttner, R. Kellermann, T. Kitahara, J. Lin, L. Leskovec, A. Lytle, M. Marshall, S. Mishima, W.G. Parrott, A. Smecca, R. Sommer, A. Soni, A. Vaquero and L. Vittorio for their input and discussions. This work is supported in part by JSPS KAKENHI Grant Number 21H01085 and by the Toshiko Yuasa France Japan Particle Physics Laboratory (TYL-FJPPL project FLAV_03).

References

[1] Y. Amhis *et al.* (Heavy Flavour Averaging Group), arXiv: 2206.07501 [hep-ex].

[2] A. Crivellin and S. Pokorski, Phys. Rev. Lett. **114** (2015) 011802 [arXiv: 1407.1320 [hep-ph]].

[3] Y. Aoki *et al.* (Flavour Lattice Averaging Group), Eur. Phys. J. C **82** (2022) 869 [arXiv: 2111.09849 [hep-lat]].

[4] A. Vaquero, PoS (LATTICE2022) 250 [arXiv: 2212.10217 [hep-lat]].

[5] E. Kou *et al.* (Belle II-Theory Interface Platform), Prog. Theor. Exp. Phys. **2019** (2019) 123C01 [arXiv: 1808.10567 [hep-ex]].

[6] E. Gulez *et al.* (HPQCD Collaboration), Phys. Rev. D **73** (2006) 074502 [arXiv:hep-lat/0601021].

[7] J.M. Flynn *et al.* (RBC/UKQCD Collaboration), Phys. Rev. D **91** (2015) 074510 [arXiv:1501.05373 [hep-lat]].

[8] J.A. Bailey *et al.* (Fermilab/MILC Collaboration), Phys. Rev. D **92** (2015) 014024 [arXiv:1503.07839 [hep-lat]].

[9] B. Colquhoun *et al.* (JLQCD Collaboration), Phys. Rev. D **106** (2022) 054502 [arXiv:2203.04938 [hep-lat]].

[10] A.X. El-Khadra, A.S. Kronfeld and P.B. Mackenzie, Phys. Rev. D **55** (1997) 3933 [arXiv:hep-lat/9604004].

[11] R.C. Brower, H. Neff, and K. Orginos, Comput. Phys. Commun. **220** (2017) 1 [arXiv:1206.5214 [hep-lat]].

[12] D. Bećirević, S. Prelovšek and J. Zupan, Phys. Rev. D **67** (2003) 054010 [arXiv:hep-lat/0210048].

[13] J. Bijnens and I. Jemos, Nucl. Phys. B **840** (2010) 54 [arXiv:1006.1197 [hep-ph]].

[14] L. Randall, M.B. Wise, Phys Lett. B **303** (1993) 135 [arXiv:hep-ph/9212315].

[15] M.J. Savage, Phys. Rev. D **65** (2002) 034014 [arXiv:hep-ph/0109190].

[16] A. Lytle *et al.* (Fermilab/MILC Collaboration), PoS (LATTICE2022) 418 [arXiv:2301.09229 [hep-lat]].

[17] J. Flynn *et al.* (RBC/UKQCD Collaboration), PoS (LATTICE2021) 306 [arXiv:2112.10580 [hep-lat]].

[18] O. Bär, Phys. Rev. D **99** (2019) 054506 [arXiv:1812.09191 [hep-lat]].

[19] S. Hashimoto, PoS (LATTICE2018) 008 [arXiv:1902.09119 [hep-lat]].

[20] O. Bär, A. Broll and R. Sommer, PoS (LATTICE2022) 402 [arXiv:2210.06857 [hep-lat]].

[21] O. Bär, A. Broll and R. Sommer, PoS (LATTICE2022) 406 [arXiv:2210.06857 [hep-lat]].

[22] L. Leskovec *et al.*, PoS (LATTICE2022) 416 [arXiv:2212.08833 [hep-lat]]

[23] K.C. Bowler *et al.* (UKQCD Collaboration), JHEP **0405** (2004) 035 [arXiv:hep-lat/0402023].

[24] R.A. Briceño, M.T. Hansen and A. Walker-Loud, Phys. Rev. D **91** (2015) 034501 [arXiv:1406.5965 [hep-lat]].

[25] R.A. Briceño, J.J. Dudek and L. Leskovec, Phys. Rev. D **104** (2021) 054509 [arXiv:2105.02017 [hep-lat]].

[26] R. Aaij *et al.* (LHCb Collaboration), Phys. Rev. Lett. **125** (2020) 011802 [arXiv:2003.04831 [hep-ex]].

[27] S. Descotes-Genon *et al.*, JHEP **1412** (2014) 125 [arXiv:1407.8526 [hep-ph]].

[28] G.P. Lepage, "The Analysis of Algorithms for Lattice Field Theory" in Boulder ASI (1989) 97.

[29] E. McLean *et al.* (HPQCD Collaboration), Phys. Rev. D **101** (2020) 074513 [arXiv:1906.00701 [hep-lat]].

[30] E. McLean *et al.* (HPQCD Collaboration), Phys. Rev. D **99** (2019) 114512 [arXiv:1904.02046 [hep-lat]].

[31] J. Harrison and C.T.H. Davies (HPQCD Collaboration), Phys. Rev. D **105** (2022) 094506 [arXiv:2105.11433 [hep-lat]]

[32] R. Aaij *et al.* (LHCb Collaboration), Phys. Rev. D **101** (2020) 072004 [arXiv:2001.03225 [hep-ex]].

[33] J. Harrison, C.T.H. Davies and A.T. Lytle (HPQCD Collaboration), Phys. Rev. D **102** (2020) 094518 [arXiv:2007.06957 [hep-lat]].

[34] J. Harrison, C.T.H. Davies and A.T. Lytle (HPQCD Collaboration), Phys. Rev. Lett. **125** (2020) 222003 [arXiv:2007.06956 [hep-lat]].

[35] R. Aaij *et al.* (LHCb Collaboration), Phys. Rev. Lett. **120** (2018) 121801 [arXiv:1711.05623 [hep-ex]].

[36] I. Bediaga *et al.* (LHCb Collaboration), arXiv:1808.08865 [hep-ex].

[37] C.M. Bouchard *et al.* (HPQCD Collaboration), Phys. Rev. D **90** (2014) 054506 [arXiv:1406.2279 [hep-lat]].

[38] C.J. Monahan *et al.* (HPQCD Collaboration), Phys. Rev. D **98** (2018) 114509 [arXiv:1808.09285 [hep-lat]].

[39] A. Bazavov *et al.* (Fermilab/MILC Collaboration), Phys. Rev. D **100** (2019) 034501 [arXiv:1901.02561 [hep-lat]].

[40] R. Aaij *et al.* (LHCb Collaboration), Phys. Rev. Lett. **126** (2021) 081804 [arXiv:2012.05143 [hep-ex]].

[41] A. Khodjamirian and A.V. Rusov, JHEP **1708** (2017) 112 [arXiv:1703.04765 [hep-ph]].

[42] R. Aaij *et al.* (LHCb Collaboration), Nature Physics **11** (2015) 743 [arXiv:1504.01568 [hep-ex]].

[43] P.A. Zyla *et al.* (Particle Data Group) Prog. Theor. Exp. Phys. **2020** (2020) 083C1.

[44] G. Duplancic and B. Melic, Phys. Rev. D **78** (2008) 054015 [arXiv:0805.4170 [hep-ph]].

[45] R.N. Faustov and V.O. Galkin, Phys. Rev. D **87** (2013) 094028 [arXiv:1304.3255 [hep-ph]].

[46] W.-F. Wang and Z.-J. Xiao, Phys. Rev. D **86** (2012) 114025 [arXiv:1207.0265 [hep-ph]].

[47] S. Aoki *et al.* (JLQCD Collaboration), Phys. Rev. D **69** (2004) 094512 [arXiv:hep-lat/0305024 [hep-lat]].

[48] J. Lin, W. Detmold and S. Meinel, PoS (LATTICE2022) 417 [arXiv:2212.09275 [hep-lat]].

[49] M. Lüscher, JHEP **1008** (2010) 071 [arXiv:1006.4518 [hep-lat]].

[50] L. Lellouch and M. Lüscher, Comm. Math. Phys. **219** (2001) 31 [arXiv:hep-lat/0003023].

[51] Z. Bai *et al.* (RBC/UKQCD Collaboration), Phys. Rev. Lett. **115** (2015) 212001 [arXiv:1505.07863 [hep-lat]].

[52] M.T. Hansen, H.B. Meyer and D. Robaina, Phys. Rev. D **96** (2017) 094513 [arXiv:1704.08993 [hep-lat]].

[53] J. Bulava, PoS (LATTICE2022) 231 [arXiv:2301.04072 [hep-lat]].

[54] P. Gambino and S. Hashimoto, Phys. Rev. Lett. **125** (2020) 032001 [arXiv:2005.13730 [hep-lat]].

[55] H. Fukaya, S. Hashimoto, T. Kaneko and H. Ohki, Phys. Rev. D **102** (2020) 114516. [arXiv:2010.01253 [hep-lat]].

[56] P. Gambino *et al.*, JHEP **2207** (2022) 083 [arXiv:2203.11762 [hep-lat]].

[57] A. Smecca *et al.*, PoS (LATTICE2022) 423 [arXiv:2211.11833 [hep-lat]].

[58] R. Baron *et al.* (ETM Collaboration), JHEP **1006** (2010) 111 [arXiv:1004.5284 [hep-lat]].

[59] A. Barone *et al.*, PoS (LATTICE2022) 403 [arXiv:2211.15623 [hep-lat]].

[60] M. Hansen, A. Lupo and N. Tantalo, Phys. Rev. D **99** (2019) 094508 [arXiv:1903.06476 [hep-lat]].

[61] G. Backus and F. Gilbert, Geophys. J. R. Astron. Soc. **16** (1968) 169.

[62] G. Backus and F. Gilbert, Phil. Trans. R. Soc. A **266** (1970) 123.

[63] H.-W. Lin and N. Christ, Phys. Rev. D **76** (2007) 074506 [arXiv:hep-lat/0608005].

[64] R. Kellermann *et al.*, PoS (LATTICE2022) 414 [arXiv:2211.16830 [hep-lat]].

[65] ATLAS, CMS an LHCb collaborations, CMS-PAS-BPH-20-003, LHCb-CONF-2020-002, ATLAS-CONF-2020-049 (CERN Report) (2020).

[66] D. Kovalskyi (CMS Collaboration), PoS (ICHEP2022) 1235.

[67] B. Colquhoun *et al.* (HPQCD Collaboration), Phys. Rev. D **91** (2015) 114509 [arXiv:1503.05762 [hep-lat]].

[68] D. Bečirević *et al.*, arXiv:1407.1019 [hep-lat].

[69] W. Lucha, D. Melikhov and S. Simula, EPJ Web Conf. **80** (2014) 00046 [arXiv:1410.6684 [hep-ph]].

[70] P. Gelhausen *et al.*, Phys. Rev. D **88** (2013) 014015 [arXiv:1305.5432 [hep-ph]].

[71] M. Black and O. Witzel, PoS (LATTICE2022) 405 [arXiv:2212.10125 [hep-lat]].

[72] A. Desiderio *et al.* (RM123+SOTON Collaboration), Phys. Rev. D **103** (2021) 014502 [arXiv: 2006.05358 [hep-lat]].

[73] D. Giusti *et al.*, PoS (LATTICE2022) 410.

[74] E. Shintani *et al.*, Phys. Rev. D **91** (2015) 114511 [arXiv: 1402.0244 [hep-lat]].

[75] K. Nakayama, T. Ishikawa and S.Hashimoto, PoS (LATTICE2019) 062 [arXiv:2001.10911 [hep-lat]].

[76] W.G. Parrott, C. Bouchard and C.T.H. Davies, Phys. Rev. D **107** (2023) 014510 [arXiv:2207.12468 [hep-lat]].

[77] W.G. Parrott, C. Bouchard and C.T.H. Davies, Phys. Rev. D **107** (2023) 014511 [arXiv:2207.13371 [hep-lat]].

[78] W.G. Parrott, C. Bouchard and C.T.H. Davies, PoS (LATTICE2022) 421 [arXiv:2210.10898 [hep-lat]]

[79] D. Du *et al.* (Fermilab/MILC Collaboration), Phys. Rev. D **93** (2016) 034005 [arXiv:1510.02349 [hep-lat]].

[80] A. Filimonova, R. Schäfer and S. Westhoff, Phys. Rev. D **101** (2020) 095006 [arXiv:1911.03490 [hep-ph]].

[81] T. Kaneko, J. Phys. Conf. Ser. **2446** (2023) 12006 [arXiv:2212.12412 [hep-lat]].

[82] T. Kaneko, X.-R. Lyu and A. Oyanguren, PoS (CKM2016) 014 [arXiv:1705.05975 [hep-ph]].

[83] B. Chakraborty *et al.* (HPQCD Collaboration), Phys. Rev. D **104** (2021) 034505 [arXiv:2104.09883 [hep-lat]].

[84] Marshall *et al.* (RBC/UKQCD Collaboration), PoS (LATTICE2022) 419.

[85] A. Conigli *et al.* (ALPHA/CLS Collaboration), PoS (LATTICE2022) 351 [arXiv:2212.11045 [hep-lat]].

[86] W. Jay (Fermilab/MILC Collaboration), PoS (LATTICE2022) 413.

[87] V. Lubicz *et al.*, Phys. Rev. D **98** (2018) 014516 [arXiv:1803.04807 [hep-lat]].